CORE
Metadata, citation and similar papers at core.ac.uk
Provided by DepositOnce

AIP Conference Proceedings

Modification of the anisotropy and strength differential effect of extruded AZ31 by extrusion-shear

Cite as: AIP Conference Proceedings **1960**, 030008 (2018); https://doi.org/10.1063/1.5034851
Published Online: 03 May 2018

M. Jaehnke, F. Gensch, and S. Mueller

View Online
Export Citation

ARTICLES YOU MAY BE INTERESTED IN

Investigation of multi-stage cold forward extrusion process using coupled thermo-mechanical finite element analysis
AIP Conference Proceedings **1960**, 030006 (2018); https://doi.org/10.1063/1.5034849

Study on numerical simulation of asymmetric structure aluminum profile extrusion based on ALE method
AIP Conference Proceedings **1960**, 030002 (2018); https://doi.org/10.1063/1.5034845

Numerical investigations on the lateral angular co-extrusion of aluminium and steel
AIP Conference Proceedings **1960**, 030001 (2018); https://doi.org/10.1063/1.5034844

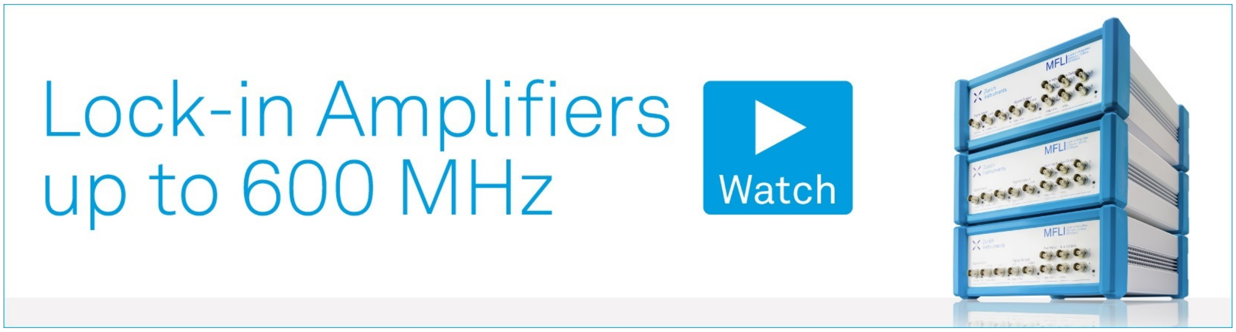

AIP Publishing

© 2018 Author(s).

Modification of the Anisotropy and Strength Differential Effect of extruded AZ31 by Extrusion-Shear

M. Jaehnke[1, a)], F. Gensch[1, b)] and S. Mueller[1, c)]

[1] *Forschungszentrum Strangpressen, Technische Universität Berlin, Gustav-Meyer-Allee 25, 13355 Berlin*

[a)] Corresponding author: martin.jaehnke@tu-berlin.de
[b)] felix.gensch@tu-berlin.de
[c)] soeren.mueller@tu-berlin.de

Abstract. The extrusion of magnesium alloys results in a pronounced fiber texture in which the basal planes are mostly oriented parallel and the c-axes are oriented perpendicular to the extrusion direction. Due to this texture the Strength Differential Effect (SDE), which describes the strength difference between tensile and compression yield strength, and the elastic anisotropy in the sheet plane are obtained during extrusion. The objective of the investigation was to decrease the SDE and anisotropy through specifically influencing the microstructure and texture. To accomplish this objective, the forming processes extrusion (EX) and equal channel angular pressing (ECAP) were combined and integrated into one extrusion die. This combination is called extrusion-shear (ES). With an ES-die, billets of the magnesium alloy AZ31B were formed into a sheet with the thickness of 4 mm and the width of 70 mm. The angles of the used ECAP-applications in the ES-dies were set to 90° and 135°. The results show that the extrusion-shear process is able to decrease the anisotropy and SDE through transformation of the texture compared to conventional extrusion process. Also grain refinement could be observed. However, the outcomes seem to be very sensitive to the process parameters. Only by using the ES-die with an angle of 135° the desired effect could be accomplished.

INTRODUCTION

During the extrusion of magnesium alloys a pronounced fiber texture develops, in which basal planes are mostly oriented parallel and the c-axes are oriented perpendicular to the extrusion direction (ED) [1, 2, 3, 4, 5]. As a result of this texture the Strength Differential Effect (SDE) [6], which describes the strength difference between tensile and compression yield strength, and the elastic anisotropy in the sheet plane during extrusion of sheet profiles are created [2, 4]. At room temperature, the basal <a>-slip and the mechanical twinning are the dominant deformation mechanisms. Under tensile loading parallel to ED, basal slip and twin formation are suppressed due the unfavorable orientation factor (basal slip) and tensile load perpendicular to the c-axis (twin), while compression parallel to ED enables easy activation of $\{10\bar{1}2\}\langle 10\bar{1}1\rangle$-extension twins. Thereby, the yield stress under compression is lower [2, 4]. The condition is similar with the anisotropy. Usually the c-axis of crystals aligns along the sheet width (TD) and thickness (ND). Crystals often form strong (0001)-pole intensities in TD and ND. As the sample orientation shifts toward TD, the orientation of the c-axis to the loading direction changes, whereby mechanical twinning at tensile loading is increasingly favored. In addition, the orientation changes beneficial for basal slip up to a certain angle. These circumstances induce a distinct lower tensile yield strength in TD than in ED. Under compressive loading, the twin formation becomes increasingly difficult with sample alignment toward TD. This effect counteracts the favor of basal slip, whereby the anisotropy under compression is lower [2]. In some cases, the c-axis aligns exclusively parallel to ND during extrusion of sheets. An approach to reduce the anisotropy and SDE is the decreasing of the average grain size [4, 5]. The Hall Petch constants for activation of twin systems are substantially larger than for activation of slip systems [7]. Due to this, the critical resolved shear stress (CRSS) for activation of twin formation increases stronger than for basal slip with decreasing grain size. However, there is a limiting factor because the texture has a stronger influence of the anisotropy and SDE than the grain size. Therefore, the objective of the

Proceedings of the 21st International ESAFORM Conference on Material Forming
AIP Conf. Proc. 1960, 030008-1–030008-6; https://doi.org/10.1063/1.5034851
Published by AIP Publishing. 978-0-7354-1663-5/$30.00

investigation is to change the texture subsequently through additional Equal Channel Angular Pressing (ECAP) integrated in the extrusion die. Mueller et. al. executed similar experiments [3]. They deformed the billet by means of a developed linear ECAP before extrusion. After 10 cycles of linear ECAP and subsequent extrusion the tensile and compression yield strength were almost equal. However, the billet had to be removed and reheated between ECAP and extrusion. Masoudpanah et. al. also showed that the texture can be influenced by the combination of extrusion and ECAP to reduce anisotropy and SDE [8]. Although they compared the shear strength in the sheet plane instead of the tensile yield strength, their results suggest, that the anisotropy is influenced by the combination of extrusion and ECAP. However, ECAP integrated in the extrusion die was first used by Orlov et. al. [9] and Hu et. al. [10] for magnesium independent of each other. Their objective was to simplify the transferability from laboratory scale to production scale and transform the discontinuous to a continuous process. Hu et. al called this principle Extrusion Shear (ES). Through the combination of both deformation processes inside one die, Orlov et. al. and Hu et. al. achieved a high grain refining as well as good balance of strength and ductility in their investigations. However, they only considered the effect on the mechanical properties under tension in ED [9, 11]. In other investigations Hu et. al. focused on 3D modelling of ES by means of finite element method [12, 13, 14]. Orlov et. al showed that the corrosion resistance increase through ES [15]. Nevertheless, both groups of scientists did not investigate the influence of ES on the anisotropy and SDE.

MATERIAL AND EXPERIMENTAL PROCEDURE

Material and Extrusion Process

The used magnesium alloy AZ31B from the company Otto Fuchs KG was homogenized for 12 hours at 350°C. The chemical composition is listened in **Tab. 1**.

TABLE 1: Chemical composition of magnesium alloy AZ31B

Al [%]	Zn [%]	Mn [%]	Mg [%]
2.9	0.78	0.25	Rest

The alloy was extruded to a sheet with the cross-sectional dimensions of 70 x 4 mm (width and thickness) at 350°C, an extrusion ratio of 25.3:1 and a ram speed of 1 mm/s. The extrudate was water quenched by a cooling ring and a water bath behind the die. The distance between bearing channel and cooling unit was about 190 mm. Due to this distance and the extrusion speed, the time in between the extrudate left the die and entered the cooling ring amounted approximately to 8 s. The used dies were a conventional extrusion die (EX-die) and an Extrusion Shear die with replaceable ECAP inserts, whereby the ECAP angle of 90° (ES-90-die, Fig. 1 a) and 135° (ES-135-die, Fig. 1 b) could be realized. Due to the modular die design, only one main body is necessary for two different ES-dies.

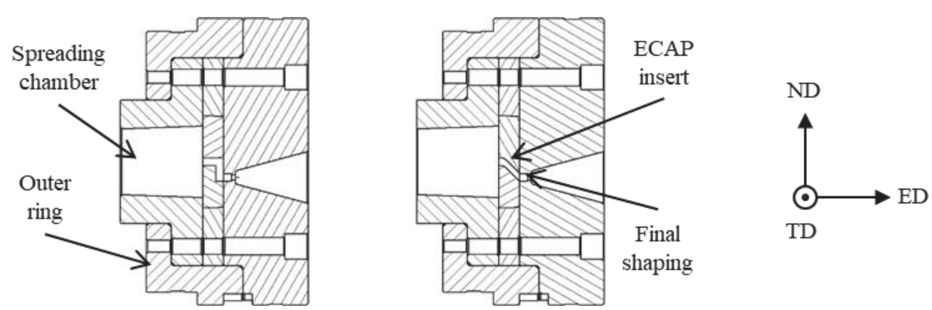

(a) (b) (c)

FIGURE 1: Used ES-Dies with channel angle of (a) 90° (ES-90) and (b) 135° (ES-135) as well as the alignment of coordinate system

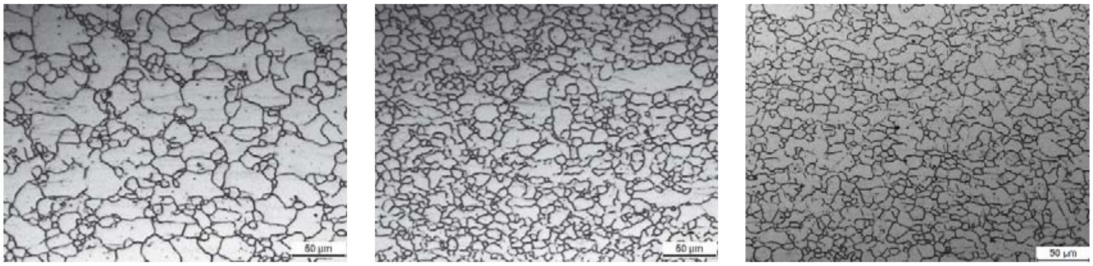

d_{av} = 23.2 µm (a) | d_{av} = 10.9 µm (b) | d_{av} = 10.5 µm (c)

FIGURE 2: Optical microscopic images taken from the center of (a) conventionally extruded the sheets, (b) ES with channel angle 135° and (c) 90°

Characterization of Microstructure and Texture

For characterization of the microstructure and texture, samples were cut from the center of the sheets. The microstructure was investigated under an optical imaging microscope (OIM) at the ND-ED-plane. Fig. 1 c shows the directions of ED, ND and TD coordinates. The texture was analyzed by means of an X-ray diffractometer (XRD) using a collimator with a diameter of 3 mm at the TD-ED-plane. Measurements were executed with monochromatic CoK_{α}-radiation (λ = 0.17887 nm) with an acceleration voltage of 40 kV. Every sample was embedded, ground and subsequently polished. The samples for microstructure investigation were additionally chemically polished with a CP2 agent consisting of 100 ml ethanol, 12 ml hydrogen chloride and 8 ml nitric acid and afterwards etched with an etching solution consisting of 70 ml ethanol, 30 ml distilled water, 15 ml acetic acid and 4.2 g picric acid.

Characterization of Mechanical Properties

The tensile and compression yield strength were determined by means of tensile and compression tests on the universal testing machine MTS 810. For the tensile tests, samples with a gauge length of 20 mm and width of 10 mm were cut and milled from the extruded sheets. The sample thickness was equal to the sheet thickness (3.67 to 3.88 mm). The samples were manufactured with the gauge length parallel to extrusion direction (ED-sample) and transversal direction (TD-sample) for consideration of the anisotropy. For the compression tests, compression samples with diameter of 3 mm and height of 5 mm were eroded from the sheets parallel to extrusion direction. The strain rate chosen for all tests was $3.6 \cdot 10^{-4} s^{-1}$.

RESULTS AND DISCUSSION

Fig. 2 shows the OIM images of the different extruded samples. It is clearly visible that a bimodal microstructure predominates in the center of all extrudates. Nevertheless, the samples of the ES-dies exhibit a finer microstructure. This indication is also confirmed through the average grain sizes dav in Fig. 2. The average grain size of the EX-sample with 23.2 µm is larger by a factor of 2.1 than the average grain sizes of the ES-135-samples (10.9 µm) and ES-90-samples (10.5 µm). Despite the theoretical higher true strain of ES-90-die resulting from the sharper ECAP angle, the ES-samples show almost the same average grain sizes.

Fig. 3 shows the calculated pole figures of {0001} basal planes and inverse pole figures in the ED from the X-ray diffraction analysis. Typical for extruded textures, all c-axes are perpendicular to the ED in the sample of EX-sheet. However, the EX-sample possessed only a ND pole and no TD component of basal planes (see Fig. 3 a). Furthermore, predominantly the $\{10\bar{1}0\}$-crystal planes lie perpendicular to ED. The low intensity of the $\langle 11\bar{2}0\rangle$-texture component shows that only a small amount of $\{11\bar{2}0\}$-crystal planes are align parallel to ED. Integrated ECAP changes the texture. In comparison to the EX-sample, some c-axes are also tilt 20° to 30° from ND to ED. This tilt is also observed in extrusion of rare-earth magnesium alloys [5, 17] and is recognizable as $\langle 11\bar{2}1\rangle$-texture component in the inverse pole figures. Occasionally, the c-axes are even parallel to ED (see Fig. 3 b). The TD pole of basal planes with similar intensity as the tilt from ND in Fig. 3 b shows, that only a few c-axes are aligned perpendicular to ED. In contrast, clearly more c-axes are oriented in TD in the ES-90-sample (see Fig. 3 c).

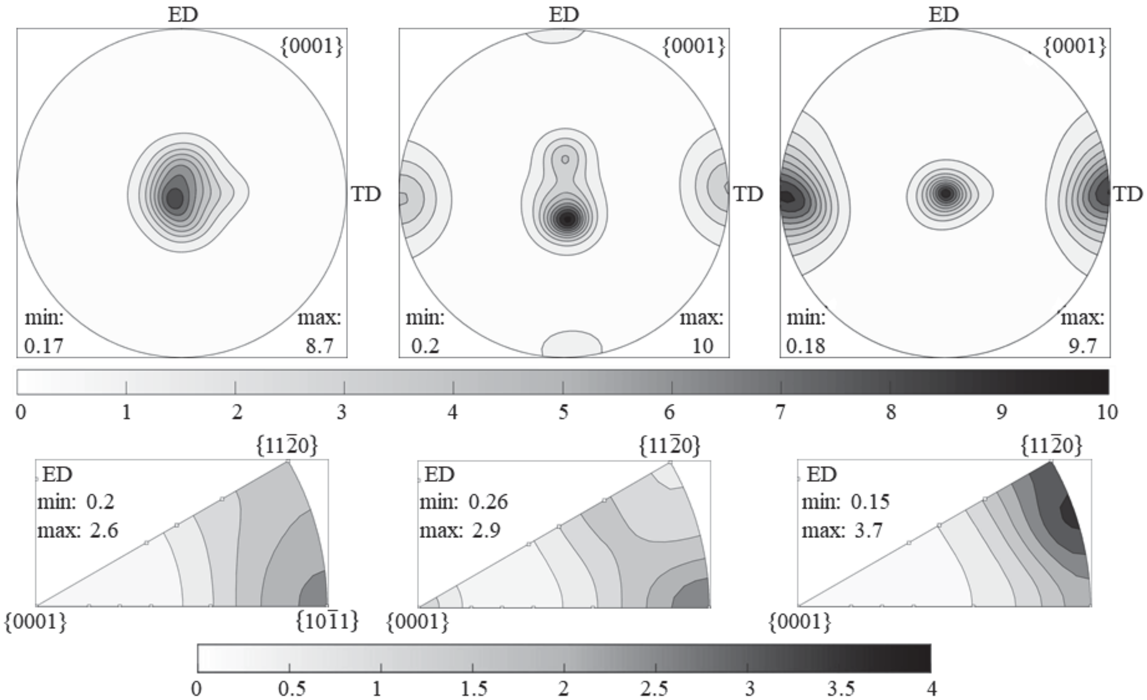

(a) (b) (c)

FIGURE 3: X-ray texture analysis of the sheets conventional extruded (a), ES with channel angle 135° (b) and 90° (c)

In addition, the basal planes of ES-90-sample have a similar intensity like that of the ES-135-sample. The typical $\langle 10\bar{1}0\rangle$-deformation is weaker pronounced in the ES-90-sample than the two other samples. Predominantly the $\{11\bar{2}0\}$-crystal planes are aligned perpendicular to ED.

The yield stress was investigated under tensile and compression load. From the individual values of compressive ($R_{C,p0,2\%}$) as well as tensile yield strength in ED ($R_{C,p0,2\%}$) and TD ($R_{t,p0,2\%,TD}$), which originate from the sheets of the different tools, average values were calculated. The SDE was determined according to equation (1) [16] and analog the anisotropy according to equation (2) with the average values.

$$\mathrm{SDE} = 2 \cdot \frac{\left(R_{c,p0,2\%} - R_{t,p0,2\%,ED}\right)}{\left(R_{c,p0,2\%} + R_{t,p0,2\%,ED}\right)} \quad (1)$$

$$\mathrm{anisotropy} = 2 \cdot \frac{\left(R_{t,p0,2\%,TD} - R_{t,p0,2\%,ED}\right)}{\left(R_{t,p0,2\%,TD} + R_{t,p0,2\%,ED}\right)} \quad (2)$$

Fig. 4 represents the results. It is noticeable that the tensile yield strengths in ED and TD of conventional extruded sheets (EX-samples) exhibit barely any differences. The average tensile yield strength in TD is slightly higher than in ED. This result arises due to the missing c-axes parallel to TD (Fig. 3 a). Tensile loading in TD does not favor tensile twins or basal slip. This leads to a positive but very small anisotropy (0.031). When compression loading is applied, a tensile stress component acts along the c-axes and tensile twins can easily be activated. Therefore, the average compressive yield strength with 97.8 MPa is well below the tensile yield strength in ED and a SDE of -0.408 results. The average tensile yield strength in ED and TD of the ES-135-samples are also almost identical, but lower than those of EX. The $\langle 11\bar{2}1\rangle$-texture component and the few c-axis parallel to ED favor the basal slip and activation of tensile twins under tension loading in ED. Therefore, the tension yield strength of the ED-samples decrease. Nevertheless, from these texture components also follows, that significantly fewer c-axes are

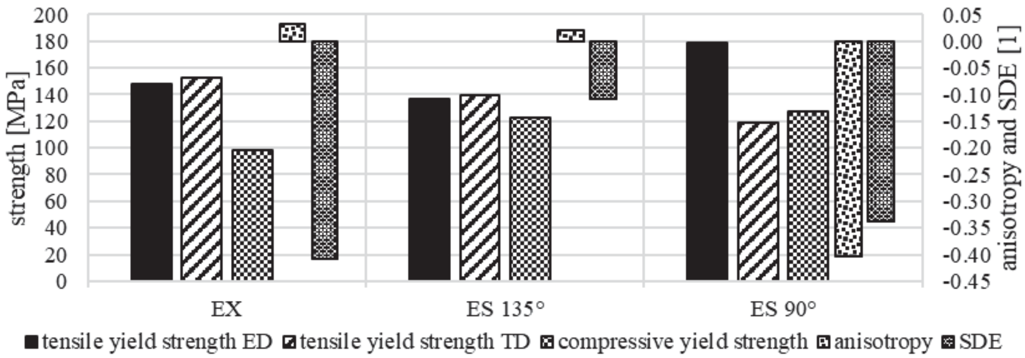

FIGURE 4: Tensile yield strength parallel (ED) and transvers to extrusion direction (TD), compressive yield strength, anisotropy as well as SDE of the sheets conventional extruded (EX), ES with channel angle 135° (ES-135°) and ES with channel angle 90° (ES-90°)

favorably orientated for activation of tensile twinning at compression loading in ED. Due to this, the average compressive yield strength with 122.5 MPa is higher than that of the EX-samples. A SDE of -0,109 follows. Through the low intensity of TD pole (Fig. 3 b) only a small amount of basal planes exhibit a beneficial alignment for basal slip or activation of tensile twins at tension loading in TD. Consequently, the ES-135-sample also shows almost no anisotropy (0.021). For the ES-90 samples, there is again a distinct anisotropy between the directions (-0.403). This anisotropy originate from the c-axes of crystals, which are always perpendicular to ED (Fig. 3 c) resulting in a high tensile yield strength of the ES-90-samples in ED (178.7 MPa) and a low tensile yield strength in TD (118.7 MPa). Similarly, the c-axes are favorable oriented for activation of tensile twins at compression loading in ED. Therefore, the ES-90-sample exhibit a clear SDE (-0.338) despite the highest average compressive yield strength of 127 MPa.

The <11$\bar{2}$0>-texture component mainly arises through elevated deformation temperature and subsequently secondary recrystallization [18, 19, 20, 21]. If the formation of the <11$\bar{2}$0>-texture component is connected with the alignment of the basal planes in TD the different textures of the samples could originate from the following reasons. The bearing length of the ES-dies is around 5 (ES-135-die) and 7 (ES-90-die) times longer than that of EX-die due the ECAP application. The resulting higher friction in the die bearing and the higher overall strain of ES leads to a larger temperature increase in comparison to conventional extrusion. The cooling rate of the water cooling at EX was high enough to mostly prevent secondary recrystallization and alignment of the basal planes in TD. However, the temperature was too high and the cooling rate too small at ES-90. Therefore, pronounced secondary recrystallization occurred and the basal planes aligned partially to TD. Since the overall strain and bearing length of ES-135-die is slightly lower than those of ES-90-die, only weak secondary recrystallization appeared. Despite of this texture, the ES-90-samples exhibit a higher tensile and compressive yield strength than the EX-samples. This circumstance is based on the Hall Petch effect, which competes with the texture induced weakening. The average grain sizes of ES samples, which are smaller by a factor of 2.1, increase the yield strength.

A comparison with other scientific works show certain similarities. Orlov et. al. [9] and Hu et. al. [11, 14] could also clearly refine the microstructure through ES. The textures in these two works show similar pole figures to those of the ES-135 sheet with slight ED contributions and tilting of the ND pole in ED basal planes. The extrusion temperatures are also at a similar level with 350°C at Orlov et. al. and 380°C at Hu et. al. In contrast, both scientist groups increase the tensile yield strength in ED. However, they did not investigate the anisotropy and SDE. [9, 11]

CONCLUSIONS

The anisotropy and Strength Differential Effect were reduced by using the ES-die with a channel angle of 135°. After extrusion with ES-135-die some c-axes are tilted from normal to extrusion direction. Some other c-axes are even aligned in extrusion direction. Therefore, the Strength Differential Effect is reduced in comparison to conventional extrusion. In addition, there is almost no anisotropy in sheets extruded with ES-135-die because only a few c-axes are oriented along the sheet width. Nevertheless, it is worth noting, that the anisotropy could also be decreased under certain circumstances at conventional extrusion. The results from the ES-90-sheet show, that the extrusion shear process is also very sensitive to the process parameters as the conventional extrusion process.

REFERENCES

1. Y. Chino; M. Mabuchi, "Influences of grain size on mechanical properties of extruded AZ91 Mg alloy after different extrusion processes", in *Advanced Engineering Materials*, 2001, Volume 3, pp. 981-983
2. S. Kleiner, P. J. Uggowitzer, "Mechanical anisotropy of extruded Mg-6% Al-1% Zn alloy", in *Materials Science and Engineering: A*, 2004, Volume 379, pp. 258-263
3. K. Müller, S. Müller, "Severe plastic deformation of magnesium alloy AZ31", in *Journal of Materials Processing Technology*, 2007, Volume 187-188, pp. 775-779
4. Y. Chino, K. Kimura, M. Hakamada, M. Mabuchi, "Mechanical anisotropy due to twinning in an extruded AZ31 Mg alloy", in *Material Science and Engineering A*, 2008, Volume 485, pp. 311-317
5. S. Gall, „Grundlegende Untersuchungen zum Strangpressen von Magnesiumblechen und deren Weiterverarbeitung: Mikrostruktur und mechanische Eigenschaften", Dr. Thesis, 2013, TU Berlin,
6. J. L. Raphanel, J. H. Schmitt, P. van Houtte, "Texture Development and Strength Differential Effect in Textured b.c.c. Metals with Glide Asymmetry", in *Materials Science and Engineering: A*, 1989, Volume 108, pp. 227-232
7. M.R. Barnett, Z. Keshavarz, A. G. Beer, D. Atwell, "Influence of grain size on the compressive deformation of wrought Mg–3Al–1Zn", in *Acta Materialia*, 2004, Volume 52, pp. 5093-5103
8. S. M. Masoudpanah, R. Mahmudi, "The microstructure, tensile, and shear deformation behavior of an AZ31 magnesium alloy after extrusion and equal channel angular pressing", in *Materials & Design*, 2010, Volume 31, pp. 3512-3517
9. D. Orlov, G. Raab, T. T. Lamark, M. Popov, Y. Estrin, "Improvement of mechanical properties of magnesium alloy ZK60 by integrated extrusion and equal channel angular pressing", in *Acta Materialia*, 2011, Volume 59, pp. 375-385
10. H.-J. Hu, D.-F. Zhang, M.-B. Yang, M. Deng, "Grain refinement in AZ31 magnesium alloy rod fabricated by extrusion-shearing severe plastic deformation process", in *Transactions of Nonferrous Metals Society of China*, 2011, Volume 21, pp. 243-249
11. H.-J. Hu, Y.L. Ying, Z.-W. Ou, X.Q. Wang, "Comparisons of microstructures and texture and mechanical properties of magnesium alloy fabricated by compound extrusion and direct extrusion", *in Materials Science and Engineering: A*, 2017, Volume 695, pp. 360-366
12. H.-J. Hu, "The Effects of Process Parameters on Evolutions of Thermodynamics and Microstructures for Composite Extrusion of Magnesium Alloy", in *Advances in Material Science and Engineering*, 2013
13. H.-J. Hu, Z. Zhai, Y.-Y. Li, H. Wang, J.-Z. Fan, Z. Ou, "3D finite Element Modeling of Grain Refinement for Magnesium Alloys by Extrusion-shear and Experimental verification", in *Materials Research*, 2014, Volume 17, pp. 1056-1064
14. H.-J. Hu, Z. Zhai, H. Wang, J.-Z. Fan, "Extrusion-shear of AZ31 alloy billets with low temperature and high speed by using three-dimensional finite element modeling and experiments", in *Materials Research*, 2014, Volume 17, pp. 987-995
15. D. Orlov, K. D. Ralston, N. Birbillis, Y. Estrin, "Enhanced corrosion resistance of Mg alloy ZK60 after processing by integrated extrusion and equal channel angular pressing", in *Acta Materialia*, 2011, Volume 59, pp. 6176-6186
16. T. B. Stoughton, J.-W. Yoon, "A pressure-sensitive yield criterion under a non-associated flow rule for sheet metal forming", in *International Journal of Plasticity*, 2004, Volume 20, pp. 705-731
17. N. Stanford, M. R. Barnett, "The origin of "rare earth" texture development in extruded Mg-based alloys and its effect on tensile ductility", *Materials Science and Engineering A*, 2008, Volume 496, pp. 399-408
18. M. T. Perez-Prado, O. A. Ruano, "Texture evolution during grain growth in annealed MG AZ61 alloy", *Scripta Materialia*, 2003, Volume 48, pp. 59-64
19. J. Bohlen, S. B. Yi, J. Swiostek, D. Letzig, H.G. Brokmeier, K.U. Kainer, "Microstructure and texture development during hydrostatic", *Scripta Materialia*, 2005, Volume 53, pp. 259-264
20. S. Yi, H.-G. Brokmeiera, D. Letzig, "Microstructural evolution during the annealing of an extruded AZ31 magnesium alloy", *Journal of Alloys and Compounds*, 2010, Volume 506, pp. 364-371
21. S. Mueller, „Weiterentwicklung des Strangpressens von AZ Magnesiumlegierungen im Hinblick auf eine Optimierung der Mikrostruktur, des Gefüges und der mechanischen Eigenschaften", Dr. Thesis, 2007, TU Berlin,